NAVSWC TR 91-492

NONDESTRUCTIVE EVALUATION OF A GRAPHITE ALUMINUM COMPOSITE SPACE RADIATOR PANEL

BY NEIL M. FELDMAN AND JOHN V. FOLTZ

RESEARCH AND TECHNOLOGY DEPARTMENT

DECEMBER 1991

Approved for public release; distribution is unlimited.

NAVAL SURFACE WARFARE CENTER

Dahlgren, Virginia 22448-5000 • Silver Spring, Maryland 20903-5000

NAVSWC TR 91-492

NONDESTRUCTIVE EVALUATION OF A GRAPHITE ALUMIMUM COMPOSITE SPACE RADIATOR PANEL

BY NEIL M. FELDMAN AND JOHN V. FOLTZ
RESEARCH AND TECHNOLOGY DEPARTMENT

DECEMBER 1991

NAVAL SURFACE WARFARE CENTER
Dahlgren, Virginia 22448-5000 • Silver Spring, Maryland 20903-5000

FOREWORD

This technical report presents nondestructive test results on a graphite fiber reinforced aluminum composite space radiator panel. The panel was evaluated after each of four fabrication stages by four nondestructive techniques: ultrasound, x-ray, dye penetrant, and visual inspection. The results illustrate the importance of nondestructive evaluation (NDE) in the qualification of materials for spacecraft application.

The funding was provided by the Naval Surface Warfare Center (NAVSWC) Weapons and Spacecraft Materials Block Program.

Appreciation is extended to Paul Brown (NAVSWC, Code R34) and Jeff Warren (NAVSWC, Code R34) for their assistance in radiography and dye penetrant testing.

The authors may be contacted at:

Naval Surface Warfare Center
Dahlgren Division, White Oak Detachment
Attn: Neil M. Feldman, Code R34
10901 New Hampshire Avenue
Silver Spring, MD 20903-5000
Phone: (301) 394-1973

Naval Surface Warfare Center
Dahlgren Division, White Oak Detachment
Attn: John V. Foltz, Code R32
10901 New Hampshire Avenue
Silver Spring, MD 20903-5000
Phone: (301) 394-2019

Approved by:

Carl E. Mueller

CARL E. MUELLER, Head
Materials Division

ABSTRACT

Graphite aluminum composites which employ graphite fibers for mechanical reinforcement have applications in the aerospace industry. They are particularly attractive for spacecraft thermal management systems due to their ability to efficiently transport heat. The detection and evaluation of damage in structures fabricated from this material is necessary to the efficiency and application of these materials.

This technical report presents research on a graphite fiber reinforced aluminum composite space radiator panel. The panel was evaluated after each of four fabrication stages by four nondestructive techniques: ultrasound, x-ray, dye penetrant, and visual inspection. The results illustrate the importance of nondestructive evaluation (NDE) from the time the composite is fabricated through the time it is implemented into the spacecraft. These NDE technologies will help detect external or internal irregularities (anomalies) at each increment of the fabrication and qualification testing of the composite radiator panel.

CONTENTS

ILLUSTRATIONS

ILLUSTRATIONS (Continued)

ILLUSTRATIONS (Continued)

INTRODUCTION

BACKGROUND

This technical report documents the nondestructive evaluation (NDE) methods used to inspect a graphite fiber reinforced aluminum (Gr/Al) composite space radiator panel. The NDE results are presented for a Gr/Al panel after primary processing, after each of the secondary fabrication operations, and after various stages of the space flight qualification testing. The Naval Center for Space Technology (NCST) designed the space radiator and conducted the flight qualification tests. The Naval Surface Warfare Center (NAVSWC) supported this project by providing the Gr/Al panels to be fabricated into radiators and performing the NDE evaluations.

COMPOSITE DESIGN

Carbon fibers made from mesophase pitch offer high stiffness, high thermal conductivity, and low density, making them an attractive reinforcement on which to base composite materials. Composite microstructural design is governed by the fabrication and service requirements of the component. For the space radiator in which the driving factor is high thermal conductivity, Amoco P120 pitch fiber was selected as the reinforcement because of its high thermal conductivity. The function of the radiator in this application is to keep the temperature of a nickel-hydrogen storage battery from exceeding a prescribed upper limit by eliminating waste heat generated during battery operation (Figure 1). Heat produced by the battery is conducted into the radiator panel by five metal webs to which the panel is mechanically attached (Figure 2). The radiator must spread the heat along its length (the 0° fiber direction) and then dissipate the heat into space.

The composite must therefore exhibit a high thermal conductivity in the 0° direction, as

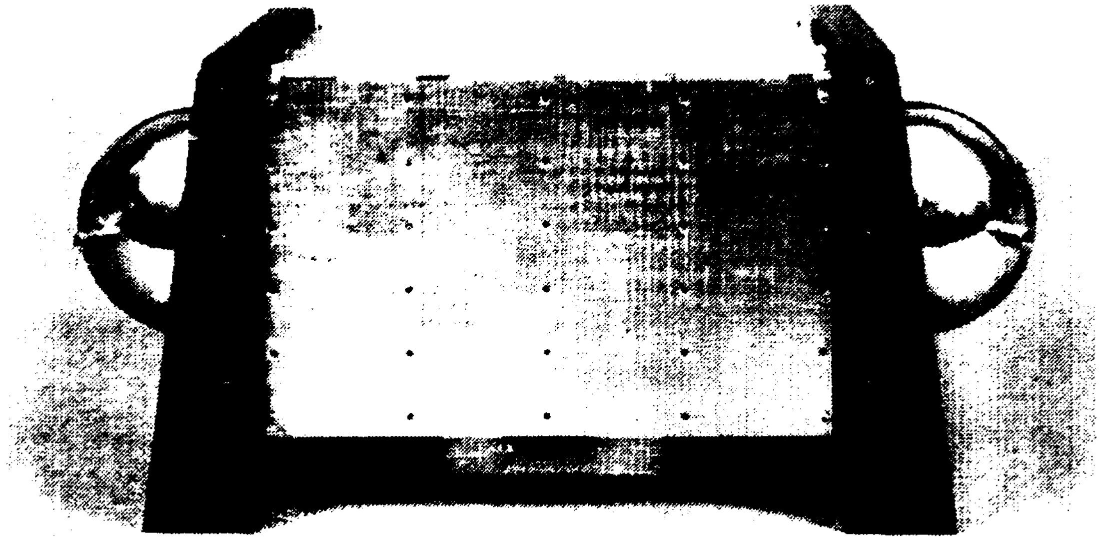

FIGURE 1. GR/AL COMPOSITE RADIATOR PANELS PROTECTING THE COMMON PRESSURE VESSEL BATTERY

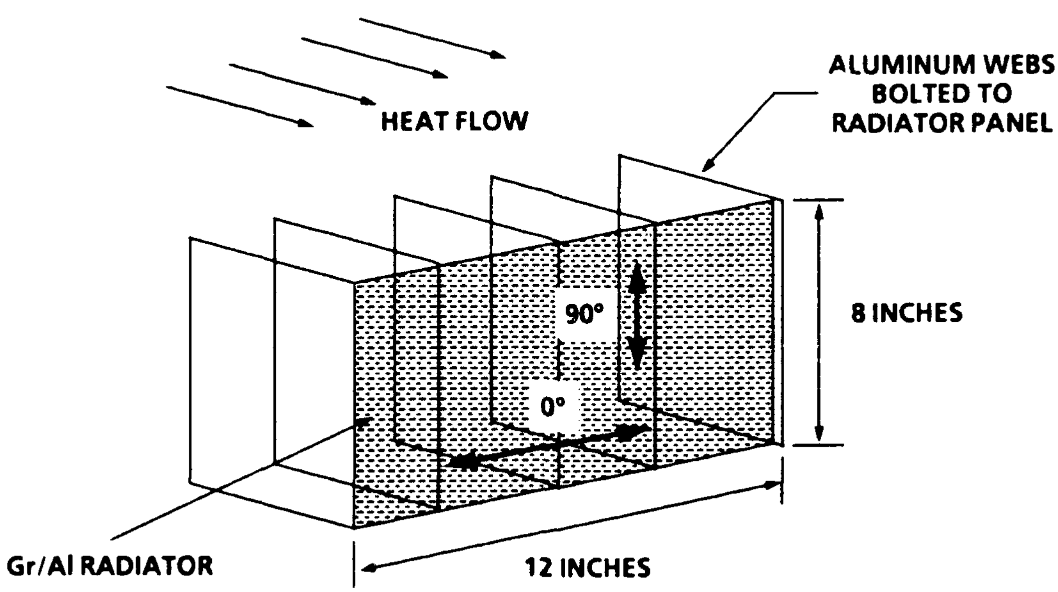

FIGURE 2. SCHEMATIC OF RADIATOR PANEL ARRANGEMENT

defined in Figure 2. Initial consideration went to using a unidirectional layup to bias the fiber arrangement in the 12-inch direction and provide the high 0° thermal conductivity needed. However, the radiator design incorporated bolt holes within one bolt diameter of the panel free edge so the composite architecture was modified to increase the strength in the 90° direction and reduce the possibility of edge tearout during machining. The configuration chosen was a $[0°_2/90°/0°_2]_{2s}$ ten-ply stack as seen in Figure 3. A 3-mil aluminum foil was added on each surface to minimize fiber print-through. This resulted in a laminate with nominal 50 mil total thickness and nominal unit ply thickness of 4.4 mil. The requested fiber fraction was 42 ± 2 percent by volume. A photomicrograph of the layup configuration can be seen in Figure 4. The white areas in the figure are the aluminum layers in the configuration. The fibers in the transverse direction are the 0° fibers used to dissipate the heat. The cross sectional fibers in the center of the micrograph are the 90° fibers which add strength to the radiator around the bolt holes.

COMPOSITE FABRICATION

DWA Composite Specialties, Inc., performed the primary processing of the P120/6061 $[0°_2/90°/0°_2]_{2s}$ panel (company number 2887) using its DWG process. The composite was produced from its raw constituents via diffusion bonding in a hot-press. Processing details were proprietary. The size of the panel delivered to NAVSWC was 12 inch by 8 inch by 0.052 inch. Secondary fabrication operations were performed by COMSAT Laboratories. COMSAT machined the perimeter cut on a high speed end mill using carbide tooling, machined the holes using high speed tungsten carbide drilling, and applied the electroless nickel coating using procedures developed for unreinforced aluminum. The plated radiator was baked at 100° C for 15 minutes.

QUALIFICATION ENVIRONMENT TESTS

The composite radiator panel was subjected to two qualification environment tests. The

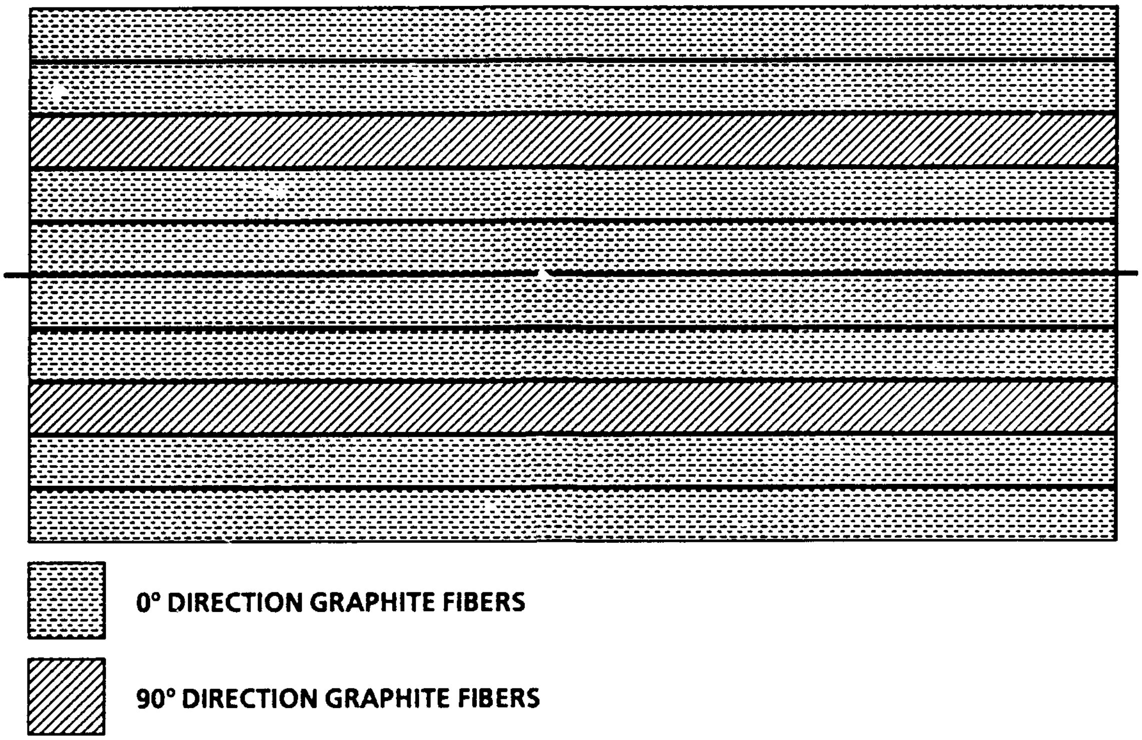

FIGURE 3. LAMINATE ORIENTATION $[0^\circ_2/90^\circ_2/0^\circ_2]_{2S}$

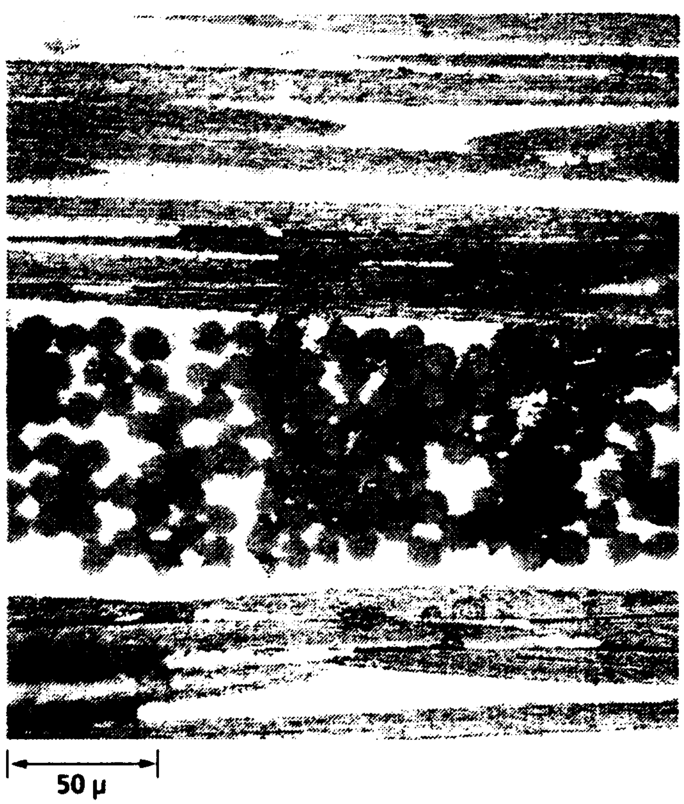

FIGURE 4. MICROGRAPH OF GR/AL PANEL

tests conducted were a vibration test and a thermal conductivity test. The vibration tests were conducted with thermal control mirrors glued to the panel and the panel attached to the common pressure vessel (CPV) battery as seen in Figure 1. The vibration qualification test frequencies for the CPV battery were between 20 Hz to 2 kHz for a duration of 120 seconds. The vibration tests were conducted for the axial and each of the two lateral directions. The vibration tests had two objectives. The first was to learn if the graphite aluminum radiator would survive the vibration tests with no visible deterioration. The second objective was to assure that the mirrors glued to the panel survived the vibration tests with no visible damage and the mirrors were still intact with the panel.

The radiator panel for qualification underwent a thermal conductivity test. The radiator had three thermal control mirrors epoxied to its surface during the test. The outboard surface of the composite radiator was covered with Kapton tape in order to improve emissivity. Min-k film heaters were installed onto a CPV battery heat sink. Thermocouples were installed on the radiator and heat sink. The assembly was placed in the thermal vacuum chamber. After pulling a vacuum and flooding the chamber shroud with liquid nitrogen, the heaters were turned on and thermocouple temperatures were monitored. The object of this test was to test the panel's thermal conductivity temperature gradient between the radiator and its respective heat sink. The thermal conductivities in the longitudinal and transverse directions were compared to the aluminum heat sink's thermal conductivities.

NONDESTRUCTIVE EVALUATION TECHNIQUES

DYE PENETRANT

Liquid penetrant inspection, a nondestructive means of locating and determining the severity of surface discontinuities in materials, is based upon fluid capillarity. Capillarity, or capillary action, attracts the fluid to the discontinuity in a concentration heavier than in the surroundings. In order for the fluid concentration to be recognized, the background area must be of sufficient contrast to distinctly reveal the defect on the surface. The sequence of the six test procedures is shown in Figure 5.

One of the most important steps of the dye penetrant procedure is the thorough cleaning of the surface area of the panel. The surface to be evaluated has to be cleaned of all scale, grease, dirt, and other foreign matter. Also, the panel should not be cleaned with much force as this would close cracks or pores that exist on the surface skin of the panel (Figure 6).

The liquid penetrant is applied to the surface of the panel in even amounts. Capillary action then draws the dye into any surface defects.[1] It is important that sufficient time (dwell time) is allowed for penetration of the dye into the surface discontinuities (Figure 7).

After the 45-minute dwell time, the excess penetrant is removed. The removal process should clean the surface of the specimen, but permit the penetrant in the discontinuities to remain (Figure 8).

The developer, which is a powder type material, acts as a blotter. The developer is applied to the surface of the panel and provides good visual contrast to the dye. The ultimate success of the liquid penetrant inspection depends upon the visibility of the indications. To ensure utmost visibility, the liquid penetrant contains a red dye easily seen in the white developer. The capillary action of the developer draws the penetrant from the discontinuity allowing the penetrant to appear on the surface of the panel as an indication. The indication,

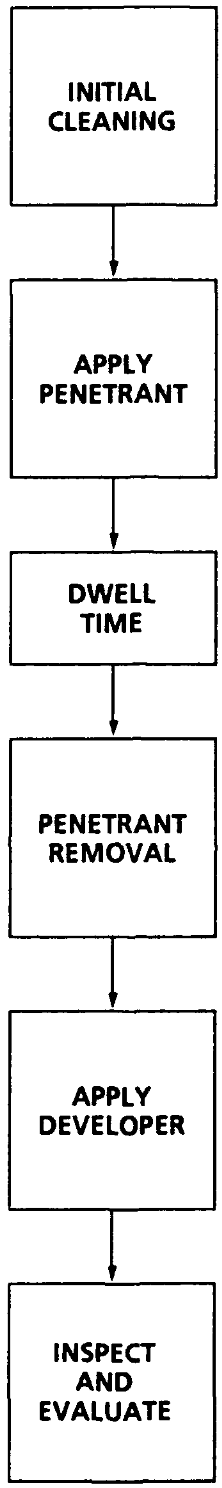

FIGURE 5. BLOCK DIAGRAM OF THE DYE PENETRANT FLAW DETECTION SYSTEM

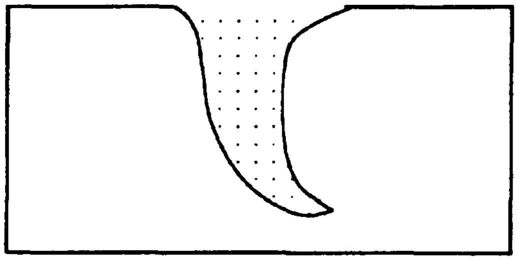

FIGURE 6. CROSS SECTION OF AN OPEN DEFECT OR IRREGULARITY

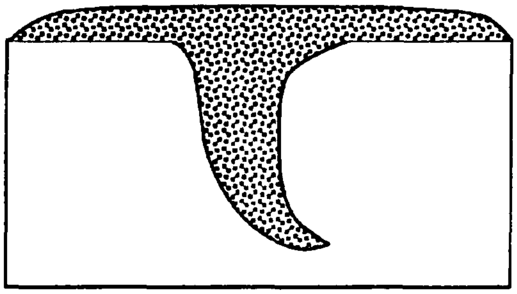

FIGURE 7. APPLIED PENETRANT, COVERING THE SURFACE AND OCCUPYING THE CAVITY

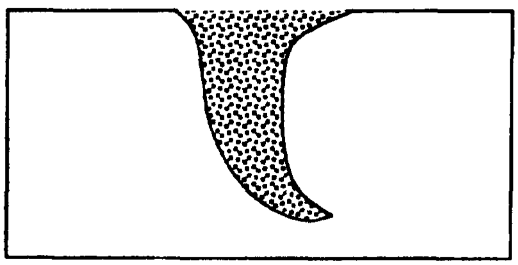

FIGURE 8. PENETRANT CLEANED FROM THE SURFACE BUT REMAINING IN THE CAVITY

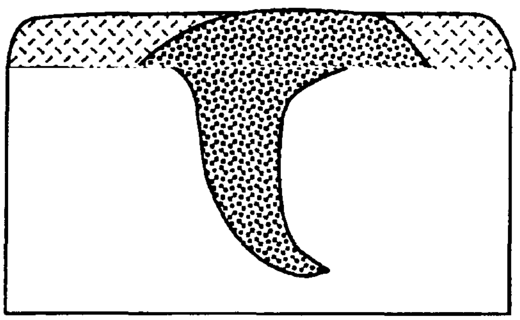

FIGURE 9. DETECTION OF THE DEFECT

because of the diffusion of the penetrant in the developer, is always larger than the discontinuity (Figure 9).

Dye penetrant inspection was conducted on the graphite aluminum composite panel after it was fabricated. There were dye penetrant indications in the 90° layup direction of the radiator. The indications were seen on the front and back surfaces of the composite. The dye penetrant method was used again after the panel was machined, and the indications were still present and had stayed constant in size. The indications were peppered (many small pin hole dots) in rows about three inches apart and about a half an inch in width as seen in Figure 10. The diameter of the dots varied. The indications seemed to be in line with the holes, and the holes made excellent reference markers for other discontinuities. After the panel was nickel-plated, the dots were still present but some seemed to be plated over while others appeared at new locations.

Each of the pinhole size dots corresponds to a pore or shallow microdimple in the aluminum. The pores were not crack-like and there were no radial crack-like indications around any of the bolt holes. The larger pores indications were approximately .02 inch in diameter, whereas most of the pore indications were approximately .005 inch in diameter (see Figure 11).

The dye penetrant method showed no new results after the qualification testing. The shallow microdimples and other surface irregularities did not change in size or depth.

RADIOGRAPHY

Radiography consists of using the penetration and differential absorption characteristics of radiant energy to examine material for internal discontinuities.[2] Figure 12 illustrates the absorption characteristics of radiation as used in the radiographic process. The composite panel absorbs radiation, but, where it is thin or where there is a void, less absorption takes place. The latent image, produced in the film, as the result of the radiation passing the panel, becomes a shadow picture of the panel when the film is processed. Generally, where the defect is an absence of material, such as a void or porosity, the image will appear darker than the

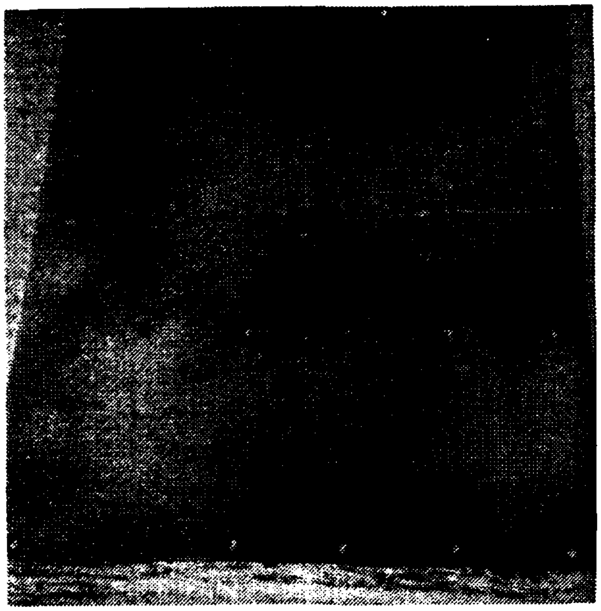

FIGURE 10. DYE PENETRANT EXHIBITING IRREGULARITIES ABOVE BOLT HOLE

FIGURE 11. DYE PENETRANT POROSITY PATTERN

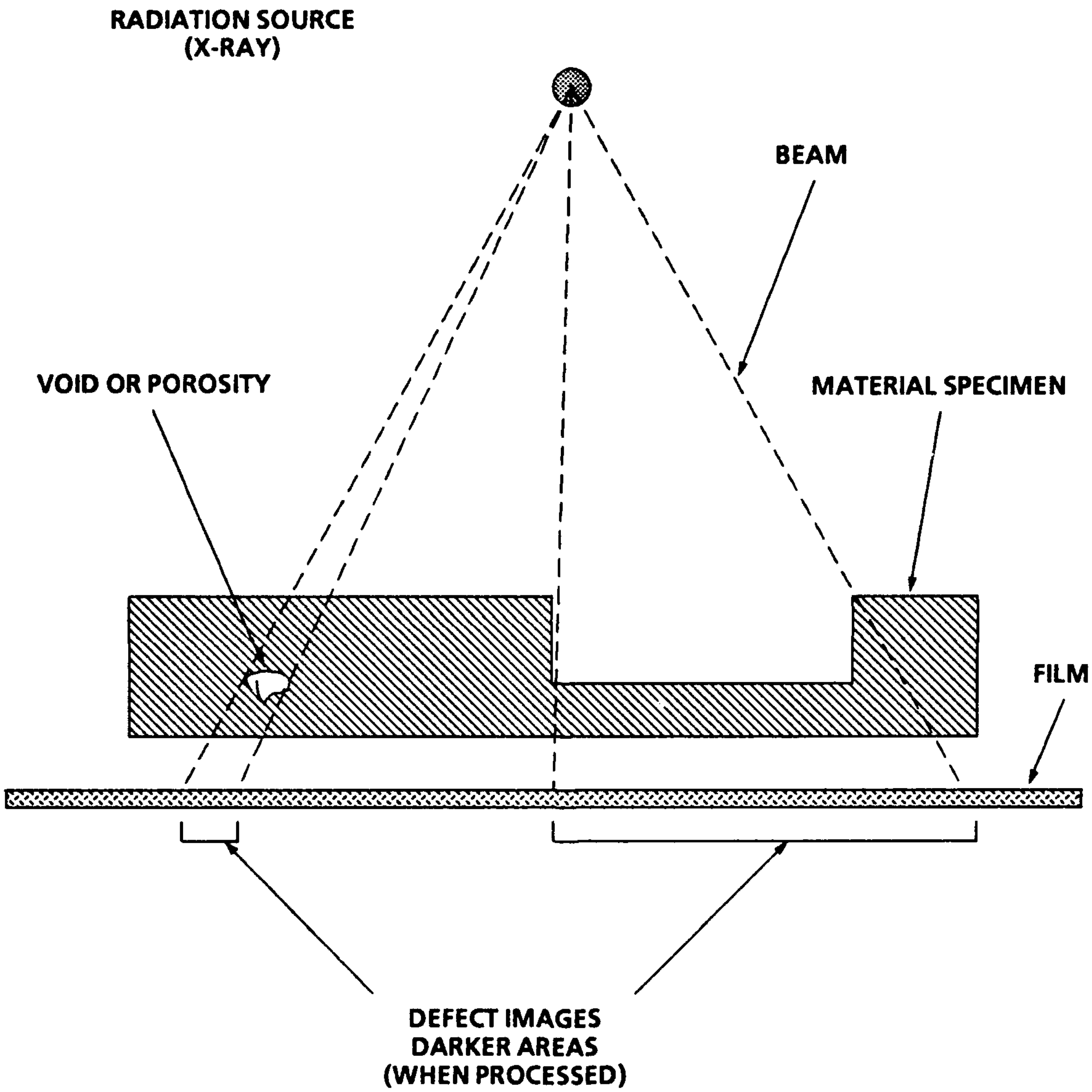

FIGURE 12. A CROSS SECTIONAL VIEW OF THE RADIOGRAPHIC PROCESS

surroundings. If the material in the defect is more absorptive than the surrounding material, the image will be lighter in appearance.

The x-ray machine utilized was the Faxitron #804. The Kodak double emulsion R film was placed approximately 24 inches from the x-ray target. The focal spot size of the x-ray beam was approximately .1 mm. The power was set at 50 kv at a current of 2.5 mA. The exposure was set for a 4-minute time cycle. The x-ray procedure was repeated after each of the fabrication steps of the composite panel.

The radiographic procedure was conducted on the composite panel at each step of fabrication and testing. The radiographic method relates atomic numbers of the material to the light and dark regions on the film at 50 kv. The dark regions correspond to a low material density (low atomic number) while the light areas correspond to a high density (high atomic number). The atomic numbers of the materials used in the composite are: carbon (atomic number of 6), aluminum (atomic number of 13), and nickel (atomic number of 28).[3] Therefore, if there is a light band within the composite, the indication could be an abundance of aluminum (the atomic number of aluminum is approximately twice that of the graphite fibers) or an absence of graphite fibers (the atomic number of graphite is approximately one half of the aluminum). If the band is dark, it would be a deficiency of aluminum or an abundance of graphite fibers or even an area of porosity. This phenomena can be seen in the radiograph in Figure 13. The graphite fiber layup can be examined by the radiograph to confirm proper layup patterns and directions.

The radiograph did not indicate any change in fiber directions or exhibit fiber breakage after the composite panel was machined as seen in Figure 13. In the radiograph, the bolt holes are black because there is no material to absorb or attenuate the x-rays. Approximately midway within the composite panel after the 3rd row of bolt holes in the 0° fiber direction, a wavy inconsistent tow of a graphite fiber can be seen. This is a layup flaw during the fabrication of the radiator. There are also pinhole black dots throughout the panel. This can be attributed to a deficiency of aluminum particles. There are some white dots on the upper right hand side of the radiograph of the panel which could be inclusion flakes of aluminum.

The radiographic method was conducted on the panel after it was nickel-plated as seen in

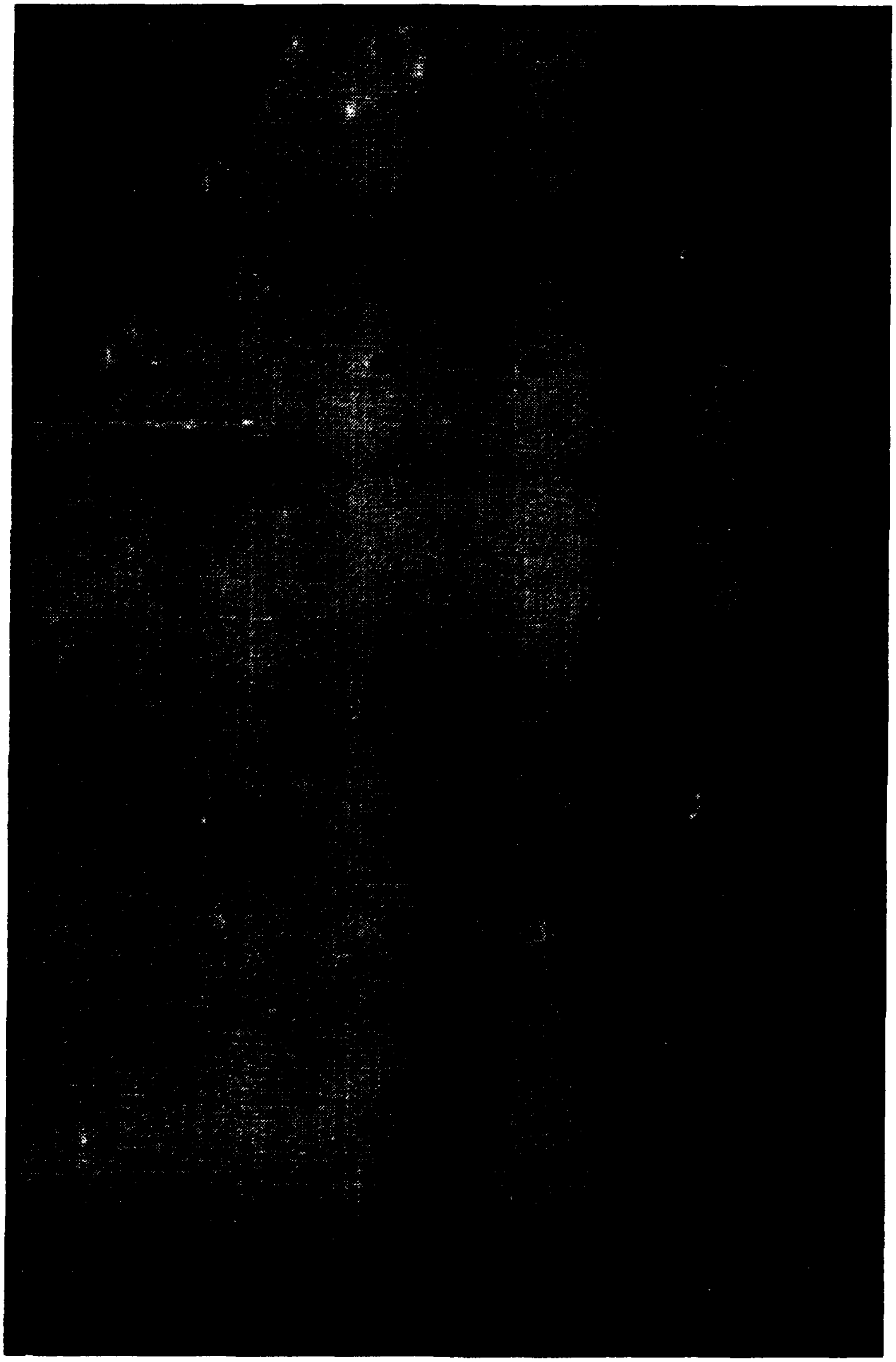

FIGURE 13. RADIOGRAPH OF COMPOSITE AFTER HOLES WERE MACHINED

Figure 14. White dots are exhibited all over the panel which can be attributed to two phenomena. The first would be that the nickel-plating process produced a very rough surface leaving small bead-type bumps on the surface of the panel. The other case for the white areas on the film is that the microdimples or pores were nickel-plated over, giving a very thin layer of nickel over the pore. The pores are filled with nickel, and since nickel has significantly higher absorption than aluminum and graphite, the nickel indications on the radiograph can be seen easily. Around the machined holes are prominent white bands which are attributed to a layer of pure nickel on the inside diameter of the drill holes (Figure 14). The nickel bands on the radiograph are an excellent method of checking the uniformity of the thickness of the nickel-plating process.

The radiograph in Figure 15, taken of the composite after the qualification tests, showed no change in the composite in comparison to the previous radiographs. Three mirrors glued to the composite appear very clear in the radiograph. The epoxy, which is the dark area shaped like a distorted square under each mirror, shows up on the radiograph in Figure 16. The black areas are areas of porosity within the epoxy.

ULTRASONIC TESTING

The ultrasonic immersion system is comprised of a flaw detection system, an ultrasound immersion tank, and computer data analysis equipment. Each component and its integrated parts will be discussed below. A block diagram of the ultrasound apparatus can be seen in Figure 17.

The flaw detection system is comprised of: a pulse generator, a receiver, an oscilloscope, a transducer, and a sweep generator. Some of these components are integrated and combined into a commercial ultrasonic test instrument. The pulse generator or pulser is the source of the short high-energy bursts of electrical energy that sets the transducer into oscillation and the trigger pulse for starting the oscilloscope display. The receiver which processes the returning echoes and initial pulse for display on the CRT is built into the flaw instrument. The straight beam immersion transducer used in the scans of the composite panel is

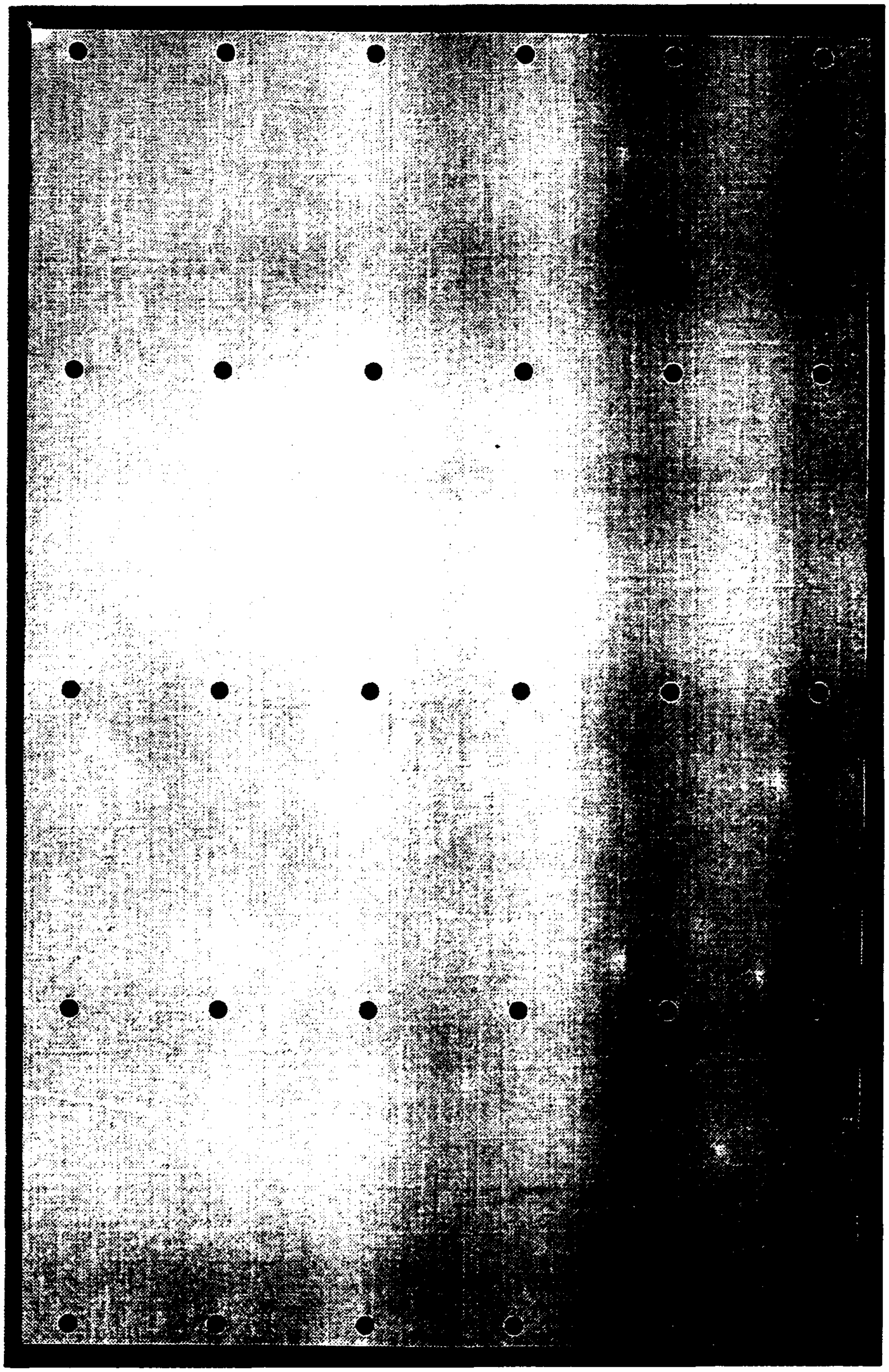

FIGURE 14. RADIOGRAPH OF COMPOSITE AFTER NICKEL PLATING

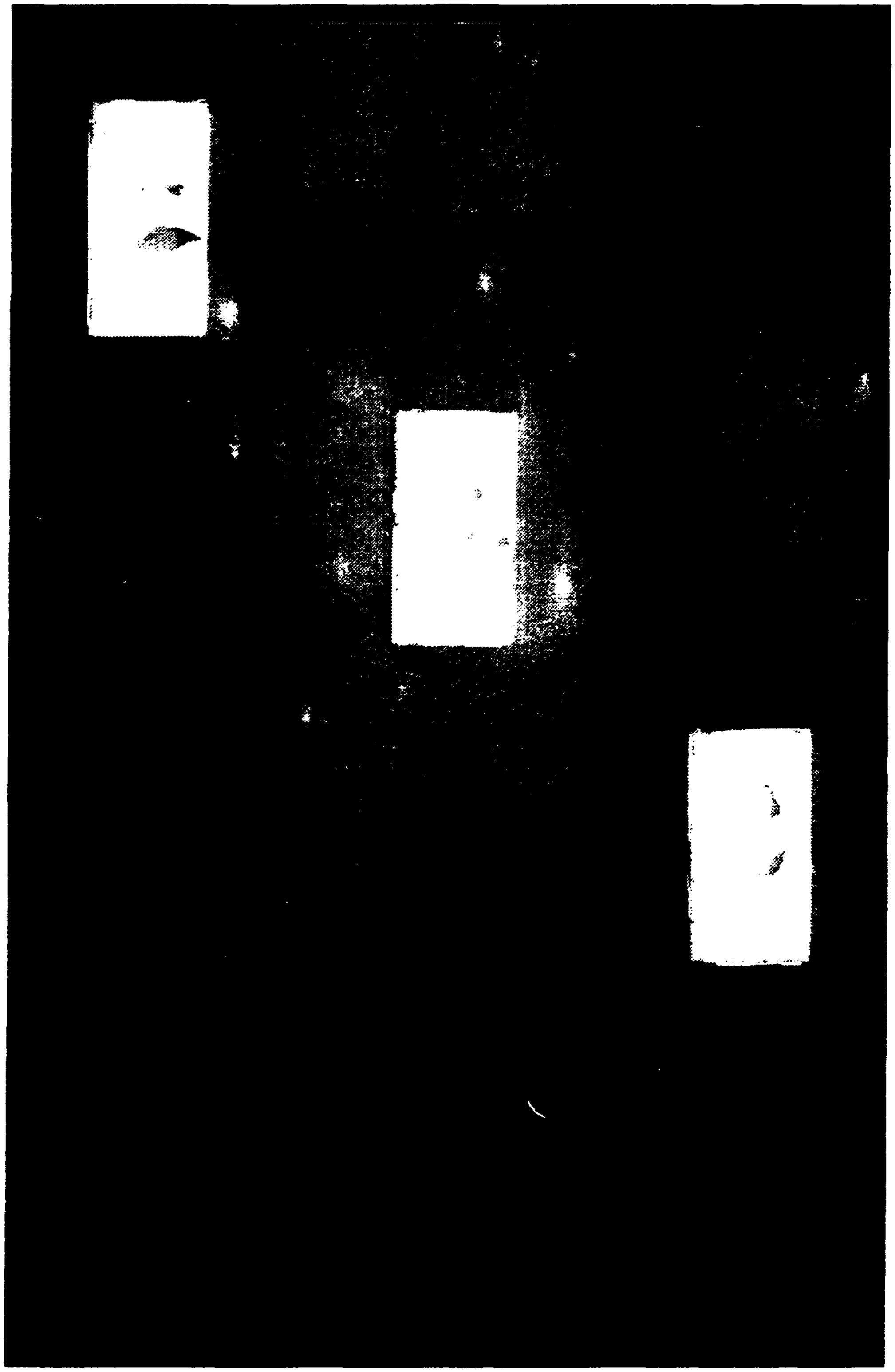

FIGURE 15. RADIOGRAPH OF COMPOSITE AFTER QUALIFICATION TEST

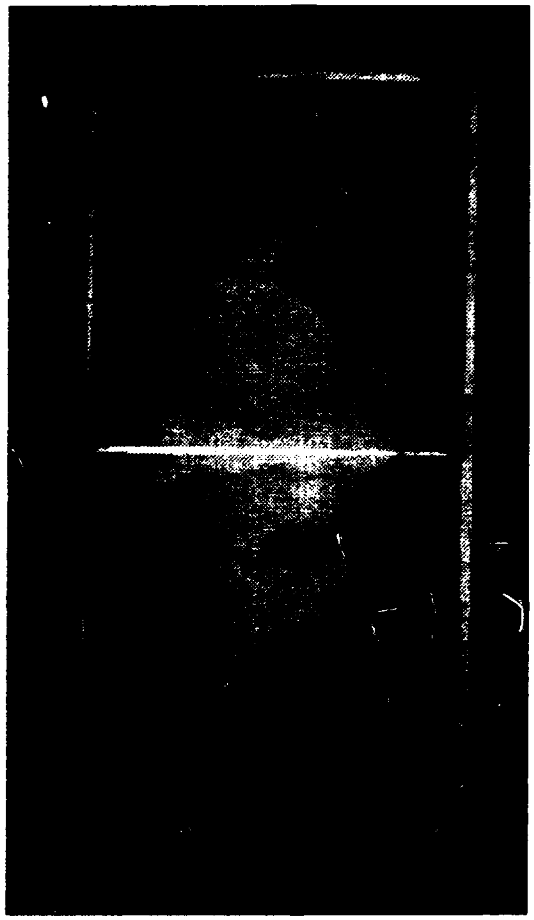

FIGURE 16. RADIOGRAPH OF THERMAL CONTROL MIRRORS

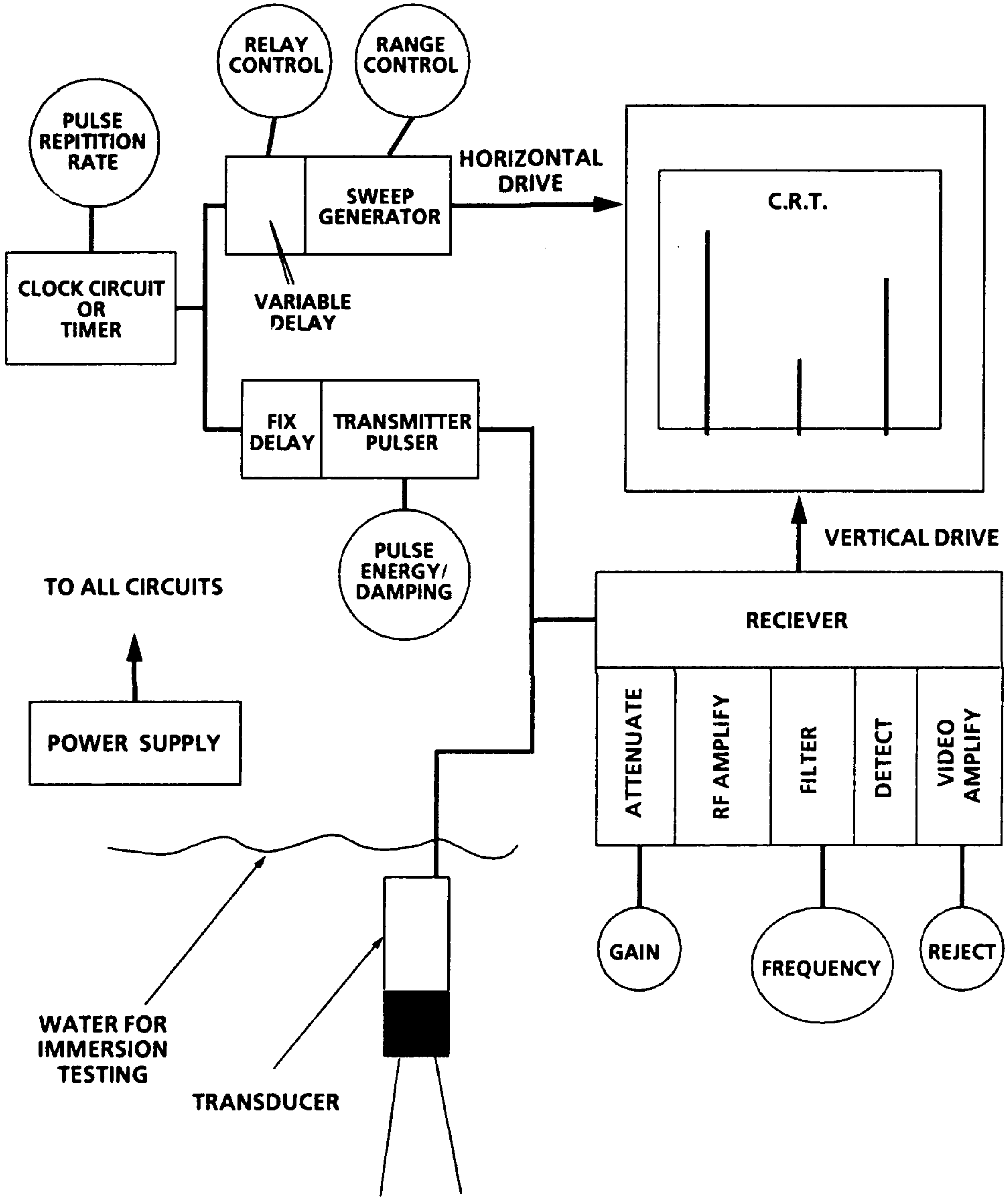

FIGURE 17. BLOCK DIAGRAM OF ULTRASONIC EQUIPMENT

a Harisonic 10 MHz, .375 inch diameter, 3-inch focused piezoelectric transducer. The beam width of the transducer at the focal point is approximately .129 inch. The transducer is focused into the composite panel for maximized resolution and flaw detection.

The immersion system is a method for automating the transducer manipulation. With this system water serves as the coupling medium between the transducer and the composite panel. The immersion system is a five-degree of freedom system. The degrees of freedom are the x, y, z, gimbal and swivel axes. The y-direction is the raster scan and the x-direction is the index for the ultrasonic image (called a C-scan). The transducer can be moved in the z-direction, hence, focusing the transducer within the composite panel. There is a wrist assembly to which the transducer is affixed that can move in a swivel and gimbal manner. The swivel is a rotation of the transducer in a 360° polar coordinate path while keeping the angle of the transducer constant. The gimbal changes the angle of the transducer. The C-scan data is taken when the transducer and the ultrasound beam are normal to the composite panel.

The A-scan is a display of the returned ultrasound signals from the composite. The A-scan which is represented by 5 sharp spikes is displayed on the CRT screen and is shown in Figure 18. The horizontal base line on the CRT indicates elapsed time (from left to right), and the vertical deflection shows signal amplitudes. These are used to determine the size of the discontinuity and the depth of the discontinuity from the front or back surface. The ultrasonic pulse echo procedure can be seen in Figure 18. The signals in Figure 18 correlate with the set-up above. The initial pulse or main bang (spike 1) travels through the water and the composite panel, and is reflected off a known reflector. Glass is chosen as a reflector (spike 4) because the material is flat with few imperfections and is an excellent reference material for repeatable results. The second spike is the front surface reflection from the composite. The portion between signal 1 and signal 2 indicates the pulse travel time in the water. Since the portion showing the water travel is of no interest, the delay and time base can be used to develop the typical A-scan display without signal 1. Therefore, the front echo (signal 2) can be located at the zero time position at the left of the screen. If there is a discontinuity (delaminations, voids, porosity) there will be a spike D after the front surface spike and before the backwall spike. The position of the discontinuity spike on the A-scan would be the position of the discontinuity

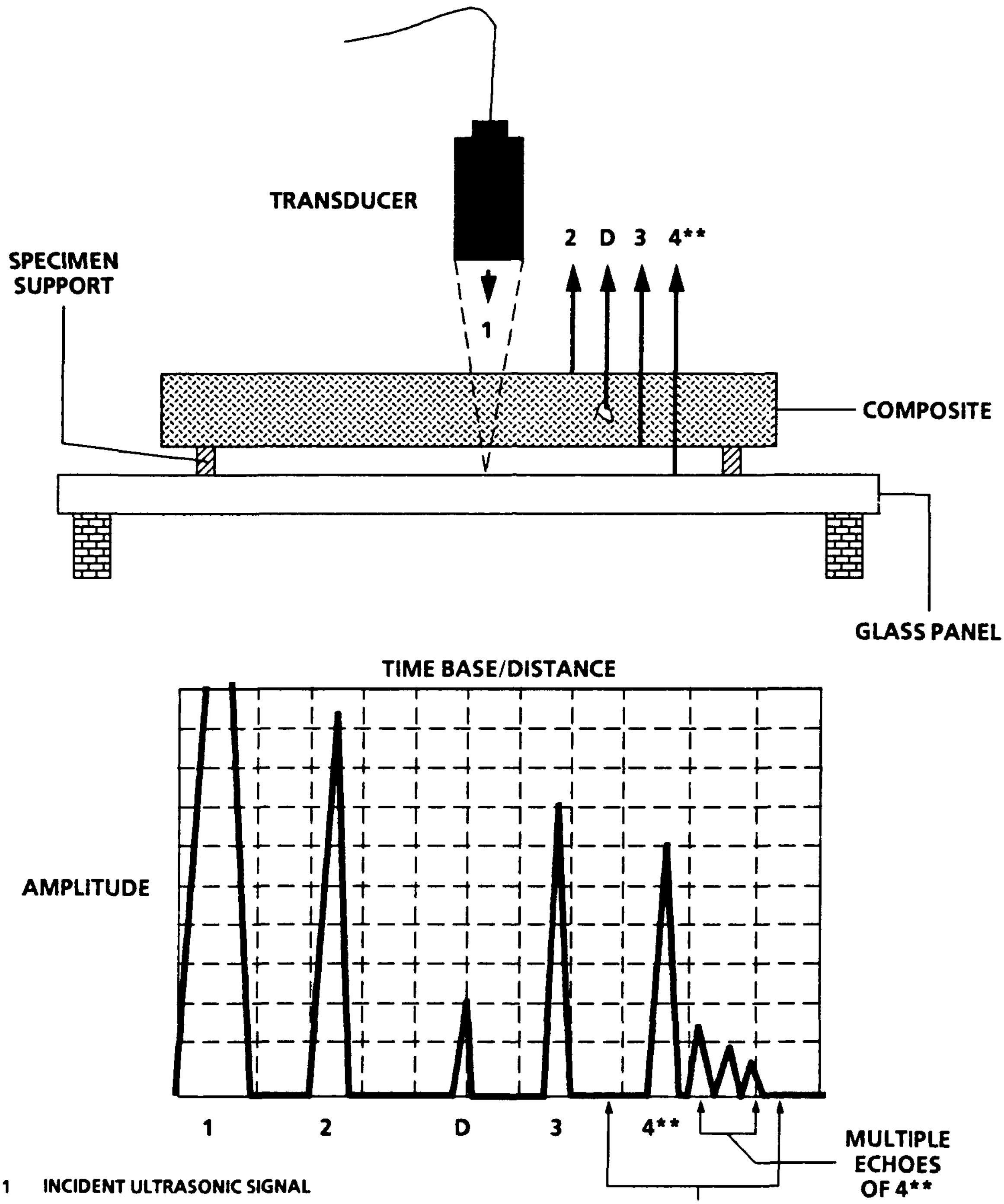

1 INCIDENT ULTRASONIC SIGNAL
2 FRONT SURFACE REFLECTION FROM COMPOSITE
D REFLECTION FROM DEFECT WITHIN THE COMPOSITE
3 REAR SURFACE REFLECTION FROM COMPOSITE
4 FRONT SURFACE REFLECTION FROM GLASS
** ELECTRONIC TIME GATE WINDOW IS PLACED TO CAPTURE THIS REFLECTION AND IS THE SIGNAL USED TO COMPRISE THE C-SCAN

FIGURE 18. DIAGRAM OF ULTRASONIC SET-UP AND A-SCAN AS SHOWN ON THE CRT OF ULTRASONIC FLAW DETECTOR

in the composite panel. The third spike is the rear surface reflection from the composite.

A C-scan is a map of the ultrasonic attenuation of the composite panel. The C-scan display is a plan view of the panel with the horizontal and vertical positions of discontinuities indicated on the printout. The C-scan provides no depth or orientation information of the discontinuities. The C-scan recording indicates the projected length and width of the discontinuity and the outline of the composite panel, as seen from directly above the panel. A window or electronic gate is used to capture the signal used for C-scan. The signal is gated on the reference glass as explained previously. A C-scan of the graphite aluminum composite panel was taken at each step of fabrication and testing as seen in Figures 19 through 25.

The computer data analysis system (MISDAC) has numerous operations in which it communicates with the immersion tank bridge. The MISDAC controls the scan and index of the bridge and all of the movements of the axes of the manipulator and transducer. The MISDAC acquires the data from the flaw detection system and digitizes the signal for advanced imaging and storage. The MISDAC acquires data from the electronic gate every .030 inch in the x and the y axis. Each voltage (range 0-10 volts) is divided into 256 levels of amplitude which is the dynamic range of the resolution of the C-scans. Other capabilities of the MISDAC include high speed grey scale and color imaging.

Corrosion is a concern in ultrasonic immersion testing of graphite aluminum composites. Water can enter the composite via the exposed sides and holes and corrode the interior of the panel. When aluminum and carbon are in contact with each other and exposed to a conductive solution (water), a potential is set up between these two materials and a current flows. Corrosion on the less corrosion-resistant material (aluminum) is increased and attack on the more resistant material is decreased, as compared to the behavior of these materials when they are not in contact. The less-resistant metal (aluminum) becomes anodic and the more resistant material (carbon) cathodic. Because of the electric currents and dissimilar materials involved, corrosion occurs.[4] This form of corrosion is a galvanic corrosion or electrochemical corrosion. The driving force for the current flow and corrosion is the potential or voltage developed between the two materials. Aluminum and carbon are very distant on the galvanic series, therefore, this combination is very vulnerable to such corrosion.

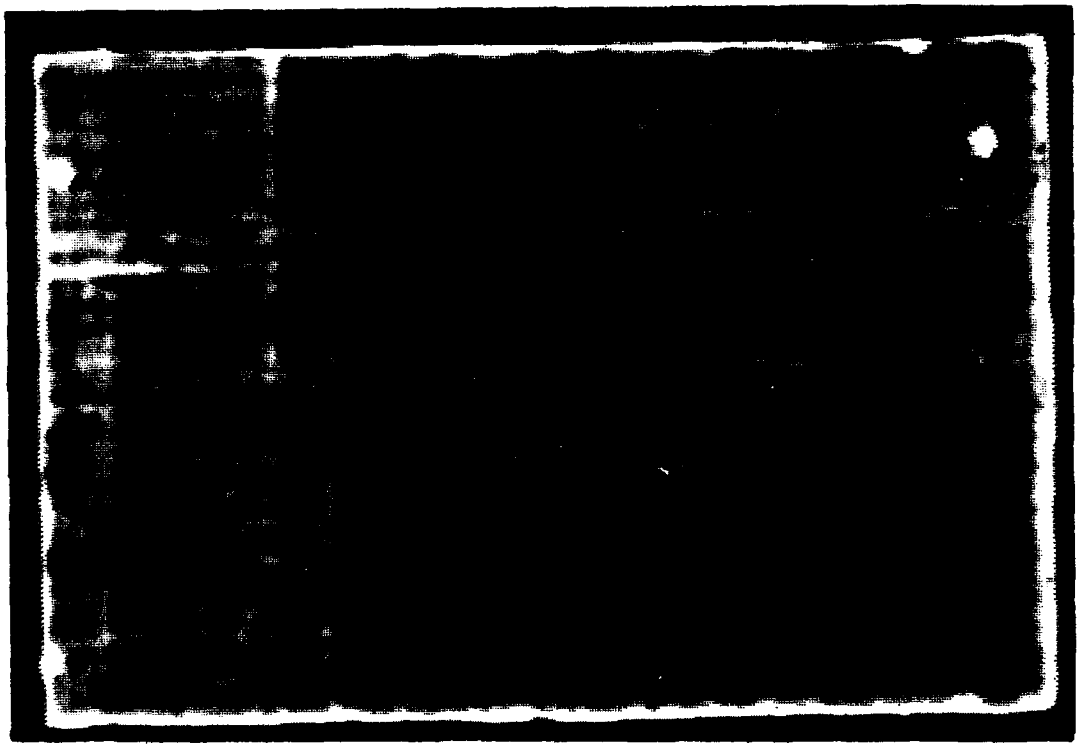

FIGURE 19. GREY SCALE C-SCAN OF PANEL AFTER FABRICATION

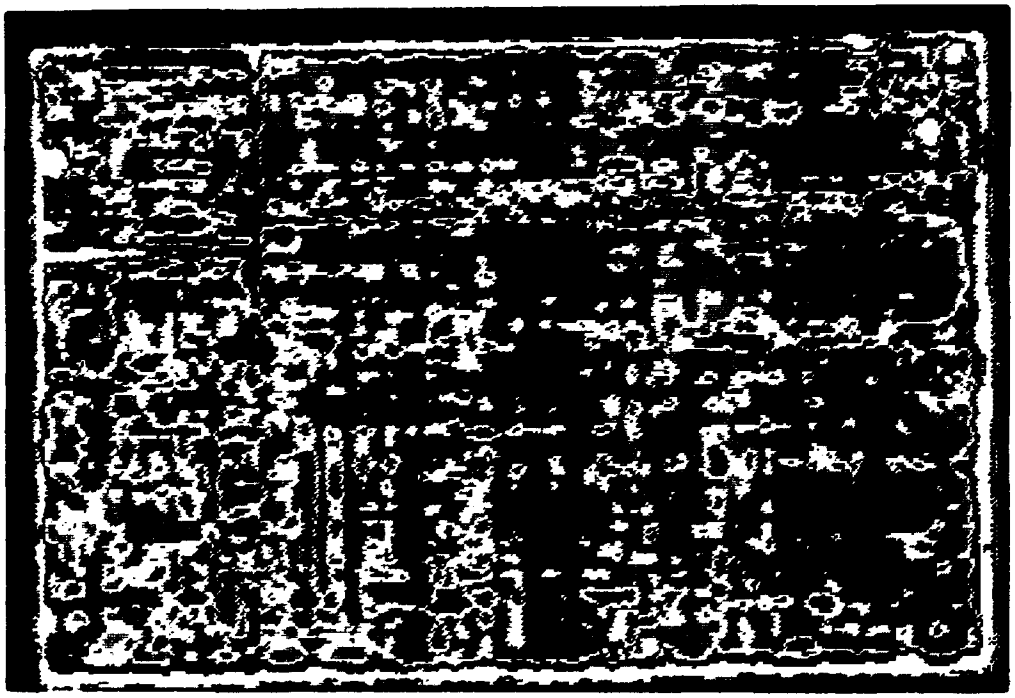

COLOR SCALE

THE C-SCANS ARE SET FOR PINK WHICH IS 50% SCREEN HEIGHT OF THE FLAW INSTRUMENT

ATTENUATED SIGNAL (db) FROM	TO	COLOR
0.0	1.5	RED/BROWN
1.5	3.0	ORANGE
3.0	4.5	DARK MAGENTA
4.5	6.0	PINK
6.0	7.5	YELLOW
7.5	9.0	BROWN/GREEN
9.0	10.5	DARK GREEN
10.5	12.0	GREEN
12.0	13.5	BLUE/GREEN
13.5	15.0	BLUE
15.0	16.5	DARK BLUE
16.5	18.0	PURPLE
18.0	19.5	WHITE

FIGURE 20. COLOR SCALE C-SCAN OF PANEL AFTER FABRICATION

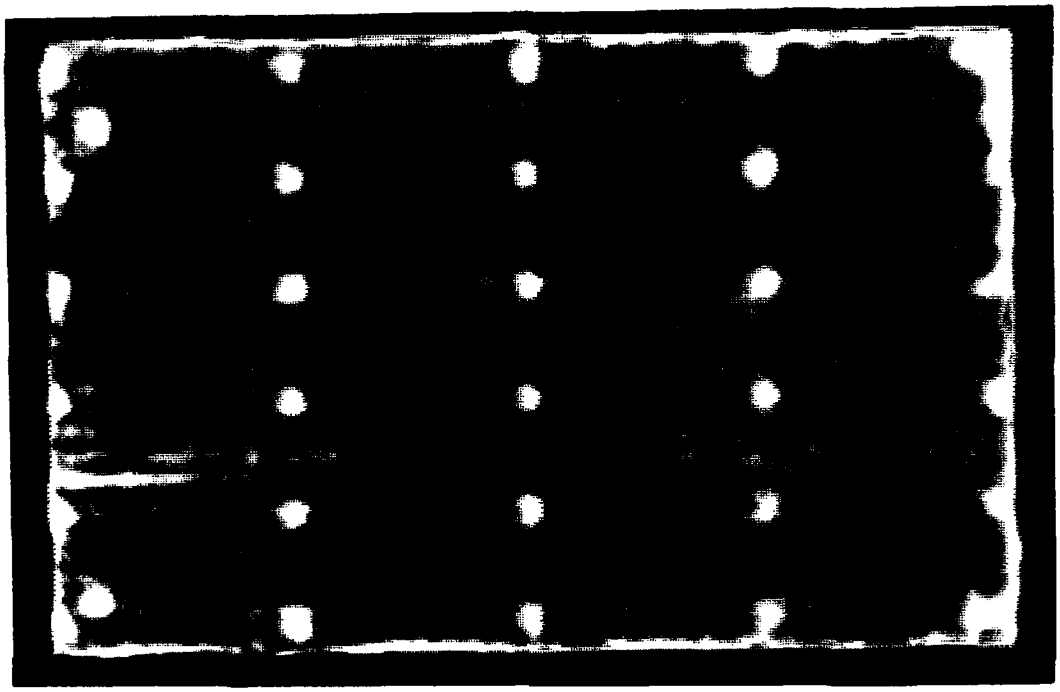

FIGURE 21. GREY SCALE C-SCAN OF PANEL AFTER HOLES WERE MACHINED

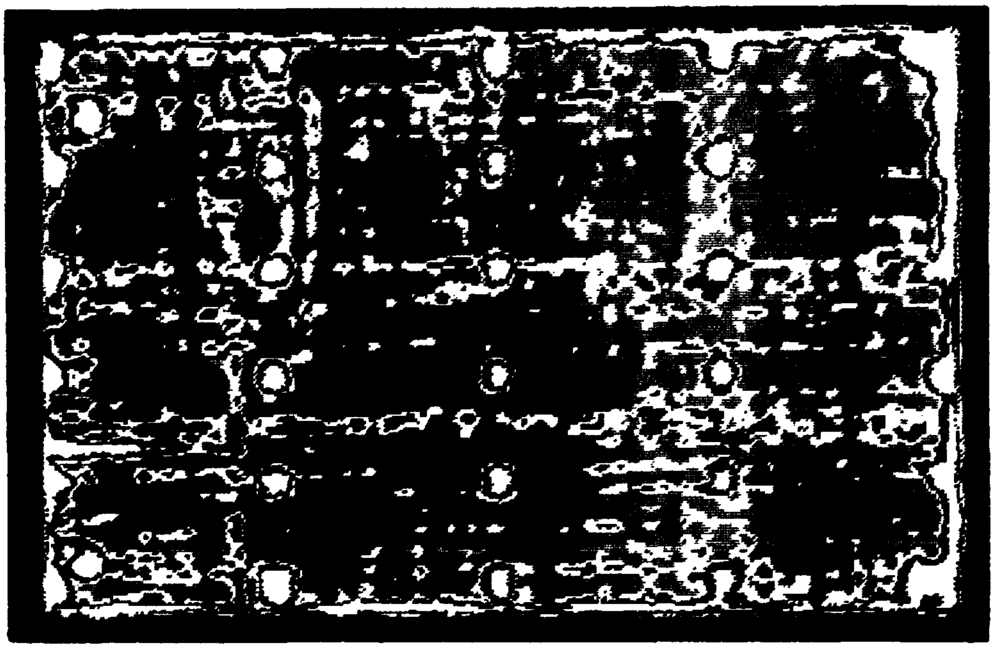

COLOR SCALE

THE C-SCANS ARE SET FOR PINK WHICH IS 50% SCREEN HEIGHT OF THE FLAW INSTRUMENT

ATTENUATED SIGNAL (db)		
FROM	TO	COLOR
0.0	1.5	RED/BROWN
1.5	3.0	ORANGE
3.0	4.5	DARK MAGENTA
4.5	6.0	PINK
6.0	7.5	YELLOW
7.5	9.0	BROWN/GREEN
9.0	10.5	DARK GREEN
10.5	12.0	GREEN
12.0	13.5	BLUE/GREEN
13.5	15.0	BLUE
15.0	16.5	DARK BLUE
16.5	18.0	PURPLE
18.0	19.5	WHITE

FIGURE 22. COLOR SCALE C-SCAN OF PANEL AFTER HOLES WERE MACHINED

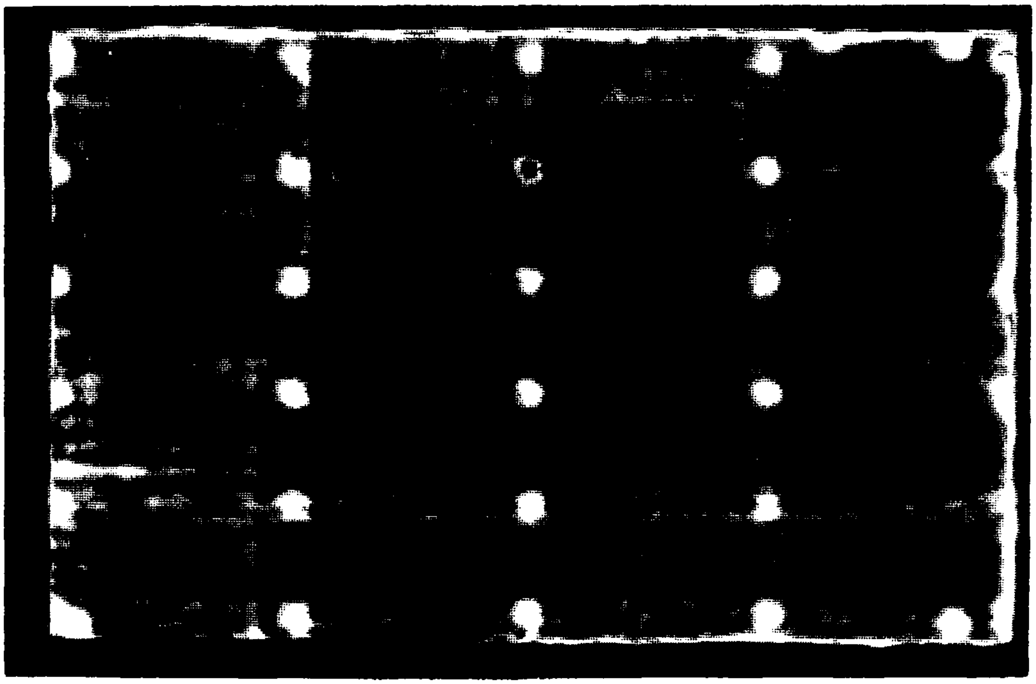

FIGURE 23. GREY SCALE C-SCAN OF PANEL AFTER NICKEL PLATING

COLOR SCALE
THE C-SCANS ARE SET FOR PINK WHICH IS 50% SCREEN HEIGHT OF THE FLAW INSTRUMENT

ATTENUATED SIGNAL (db)		
FROM	TO	COLOR
0.0	1.5	RED/BROWN
1.5	3.0	ORANGE
3.0	4.5	DARK MAGENTA
4.5	6.0	PINK
6.0	7.5	YELLOW
7.5	9.0	BROWN/GREEN
9.0	10.5	DARK GREEN
10.5	12.0	GREEN
12.0	13.5	BLUE/GREEN
13.5	15.0	BLUE
15.0	16.5	DARK BLUE
16.5	18.0	PURPLE
18.0	19.5	WHITE

FIGURE 24. COLOR SCALE C-SCAN OF PANEL AFTER NICKEL PLATING

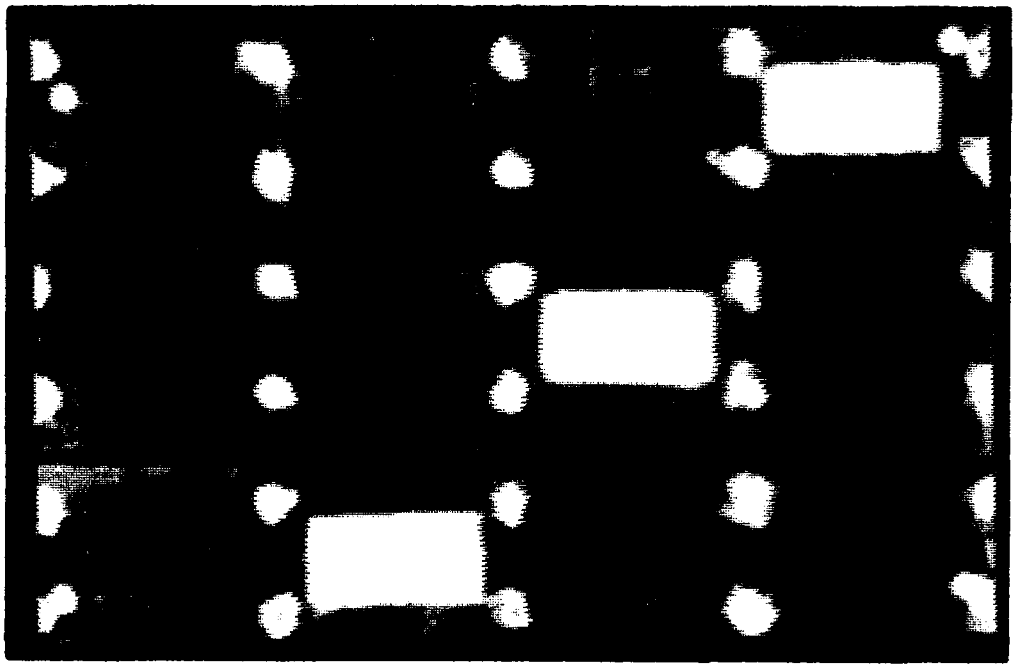

FIGURE 25. GREY SCALE C-SCAN OF PANEL AFTER QUALIFICATION TEST

The contents of a delamination (separation of composite layers) and a void is air. The void and delamination are indicated on the C-scan by way of their very high attenuation of their ultrasound signal. Ultrasound cannot pass through air, but when water replaces the air in these defects, the attenuation is reduced. This reduces the change in signal used to indicate a void or delamination, thus giving a false evaluation of the panel. Therefore, because of the galvanic corrosion and the ultrasound phenomena above the panel edges need to be protected from the water of the ultrasonic immersion tank.

A method of water proofing or sealing these exposed edges of the composite is achieved by a silicone adhesive (RTV). The adhesive is applied to the edges by a fine tip brush and takes approximately 24 hours to setup and cure. Once the adhesive has been cured it seals the surface from moisture. The silicone adhesive will highly attenuate the ultrasound waves as seen on the outer edges and the holes in the C-scans in Figure 19. Therefore, special care must be taken not to spread the adhesive on unexposed areas. When the ultrasound tests are completed the silicone adhesive can be peeled away from the composite with no left over residue.

A grey scale is used for the C-scans which were conducted on the composite panel. The white represents a high signal attenuation while the black represents no signal attenuation (as if the material were transparent). White bands can be seen around the perimeter of the panel which are high attenuation areas of the RTV adhesive. On the corners of the panel are four white holes which are spacers that support the composite above the reference glass. These spacers should be ignored on the C-scans. A 14-color scale is also used for the C-scans conducted on the panel. Each color represents a range of voltages. If a signal falls into a parameter of a voltage, the signal is assigned a color which corresponds to that parameter. Each adjacent color is a change of approximately 1.5 dB.

The C-scan in Figures 19 and 20 has some irregularities within the panel. The 0° and 90° fiber directions can be seen in the C-scans. There is approximately a 3 to 4.5 dB attenuation difference in signals between some of the regions within the panel. On the left side of the panel there are areas exhibiting approximately 8.5 dB additional attenuation. Visual inspection of the panel edges, on this side revealed delaminations. In Figure 20 starting from the upper left side of the panel is a white spike which appears to be a delamination evaluated from the ultrasound data and visual inspection. This area is where the entire signal is attenuated approximately 19 dB. In Figures 21 and 22, the holes can be seen in the C-scan after the panel has been machined. The holes are white because of the RTV adhesive attenuating the ultrasound signal. The panel for Figures 21 through 25 is rotated 180° around the 0° axis changing the orientation of the C-scans, but leaving the ultrasound parameters unchanged. This change in orientation occurred because the reference number on the panel was cleaned during the machining process, and Ni plated over. In Figure 22 the delaminations in the left region of the panel appeared to be reduced in severity in the C-scan. But, the delamination in the left side of the panel is unchanged in its signal attenuation. The center and right region of the panel is more homogenous in signal strength, areas of anomalies seem to have lessened in severity. The reasons for this phenomenon will be represented in the discussion. From the C-scan the panel appears to be in good structural shape.

The C-scans in Figures 23 and 24 were conducted after the panel went through the process of being nickel plated. The panel appeared to be unchanged from the nickel-plating process.

The C-scan in Figure 25 was conducted after the thermal conductivity and the vibration tests. There are three large reflecting mirrors glued to the panel which could not be removed. The three mirrors show up as three white squares which should be ignored in the C-scan. The panel appeared to be unchanged after the qualification environment tests.

DISCUSSION

The composite panel's soundness appeared to improve in the subsequent C-scans after the holes were machined. A hypothesis is that this phenomena is attributed to the panel's physical layup properties during fabrication. When the composite is fabricated a residual stress is created by the aluminum shrinking and the graphite fiber tending to remain in its original form during the cool down process. The graphite fibers are under compression while the aluminum is under tension. When the holes are machined there is a relaxation of the membrane stresses in both materials created by the free surface around the holes and decreasing with distance from the free surface. If there is a delamination within the composite the delamination could lead to a bending moment between layers. When some of the compression is released by the drill holes the relaxation allows the delamination to close.

It was thought that the water from the ultrasound tank was penetrating the panel through its exposed surfaces between the silicone adhesive and aluminum interface by capillary action. The delamination starting from the left side of the panel was present in the fabrication scan and the scans preceding the machining process. The signal comes into contact with the left edge of the panel and an edge of a drill hole. If water could have penetrated into the panel from an edge or an edge hole, this signal would also be affected. From the results of this delamination and in Appendix A, the occurrence of water penetration is unlikely. Therefore, the phenomena of the C-scans appearing to improve, are possibly from the residual stresses within the panel being released by the drill holes.

SUMMARY

Nondestructive evaluation is very important from the time the composite is fabricated through the time it is used for its application. A combination of NDE technologies is used to evaluate the graphite aluminum composite space radiator panel.

The surface of the panel had some irregularities (porosity) on the aluminum faces. The dye penetrant method showed this in the panels before and after the machining and nickel-plating.

Radiographic NDE exposed areas of surface roughness and showed that the nickel was plated over the porosity created in the fabrication of the panel. Radiographic NDE proved to be an excellent method of checking the uniformity of the thickness of the nickel plating process. From the radiograph's verification of the location of a inconsistent tow and some layup anomalies in the 0° fiber direction within the composite are achieved. Radiography is useful in the inspection of the uniformity of the epoxy used to adhere the thermal control mirrors to the face of the radiator panel. The radiographs showed areas of porosity in the epoxy which could inhibit the effectiveness of the epoxy's ability to conduct heat and its effectiveness in adhering the mirrors to the face of the panel.

The ultrasound C-scans provided important data about the interior of the radiator panel. The C-scans exhibited areas of delaminations and anomalies within the panel. The composite panel's soundness appeared to improve in the subsequent C-scans after the holes were machined. The hypothesis is that when the holes are machined there is a relaxation of the membrane stresses in both materials created by the free surface around the holes and decreasing with distance from the free surface. The relaxation after the machining of the drill holes allowed the delamination to close resulting in a lower attenuated signal in the C-scans. The panel appeared to be unchanged from the nickel-plating process and after the qualification environment tests.

The panel's internal and external integrity as demonstrated by the dye penetrant, radiographic and ultrasonic evaluations was not impaired by the fabrication process and two space qualification environment tests, which included both vibration and thermal cycling.

REFERENCES

1. Bray, Don E. and Stanley, Roderic K., *Non Destructive Evaluation*, McGraw Hill Book Co., Inc., New York, NY, 1989, pp. 479-500.

2. Knoll, Glenn F., *Radiation Detection and Measurement*, John Wiley & Sons, Toronto, 1979, pp. 421-427.

3. Brodsky, Allen B., *Handbook of Radiation Measurement and Protection*, CRC Press Inc., West Palm Beach, FL, 1978.

4. Bosich, Joseph F., *Corrosion Prevention for Practicing Engineers*, Barnes & Noble Inc., New York, NY, 1970, pp. 24-29.

BIBLIOGRAPHY

Booth, R.C., et al., "Techniques for Cleaning Test Objects Surfaces," in R. C. McMaster (ed.), *Nondestructive Testing Handbook*, Vol. 2, Liquid Penetrant Tests, 2d ed., American Society for Metals, Materials Park, OH, 1982, sec. 2.

Dobbs, E.R., "Electromagnetic Generation of Ultrasound," in R.S. Sharpe (ed.), *Research Techniques in Nondestructive Testing*, Vol II, Academic, London, 1973, Chap. 13.

DOD/NASA Advanced Composites Design Guide, Contract F33615-78-C-3203, Rockwell International, Flight Dynamics Laboratory, Wright Patterson Air Force Base, July 1983.

Emigh, C.R., "Radiation and Particle Physics," *Nondestructive Testing Handbook*, Vol. 3, Radiography and Radiation Testing, 2d ed., American Society for Nondestructive Testing, Columbus, OH, 1985, Sec. 1, pp. 62-90.

Krautkramer, J. and Krautkramer, H., *Ultrasonic Testing of Materials*, 3d ed., Springer-Verlay, Berlin, 1983.

Martin, B.G., "Some Techniques for Nondestructive Evaluation of Graphite Fiber Reinforced Composites," *Society of Manufacturing Engineers*, EM 78-402, 1978.

McKague, E.L., Haklias, J.E. and Reynolds, J.D., "Moisture in Composites," *Journal of Composite Materials*, Jan 1975, Vol. 9, p. 2.

BIBLIOGRAPHY (Continued)

Mulroy, B.J. and Mazenko, D.M. (Lockheed), "Adhesive Bonding for Space Applications," *SAMPE Symposium*, New York, NY, Oct 1978, Vol. 10, p. 416.

Poursartip, A., Ashby, M.F. and Beaumont, P.W.R, "The Fatigue Damage Mechanics of a Carbon Fiber Composite Laminate: Life Protection," *J. Compos. Sci. Technology*, Vol. 25, 1986.

Robinson, S.J. and Schmidt, J.T., "Fluorescent Penetrant Sensitivity and Removability - What the Eye Can See, a Fluorometer Can Measure," *Materials Evaluation*, Vol. 42, No. 8, Jul 84, pp. 1029-1034.

Schoutens, J.E., "Introduction to Metal Matrix Composites," Tutorial Series No. 272, Metal Matrix Composites Information Analysis Center, June 1982.

Silk, M.G. and Lidington, B.H., "A Preliminary Study of the Effect of Defect Shape and Roughness on Ultrasonic Size Estimates," *Nondestructive Testing*, Vol. 8, No. 1, Feb 75, pp. 27-31.

Sturges, D.J., "Quality - The Critical Challenge," *The Leading Edge*, (General Electric Company, Cincinnati, OH), Fall 1985, pp. 2-7.

APPENDIX

EXAMPLE OF WATER DIFFUSION INTO A GRAPHITE ALUMINUM COMPOSITE PANEL

A graphite aluminum composite panel with known gross delaminations was submerged into the ultrasound tank without the silicone adhesive. The signal attenuation of a particular spot within the delamination was observed and recorded. As time elapsed water entered the delamination, hence water replaces air giving a path for the ultrasound signal to travel. This would give a false C-scan for the delamination because the signal is no longer being attenuated by air. The plot of water diffusion versus signal attenuation can be seen in Figure A-1.

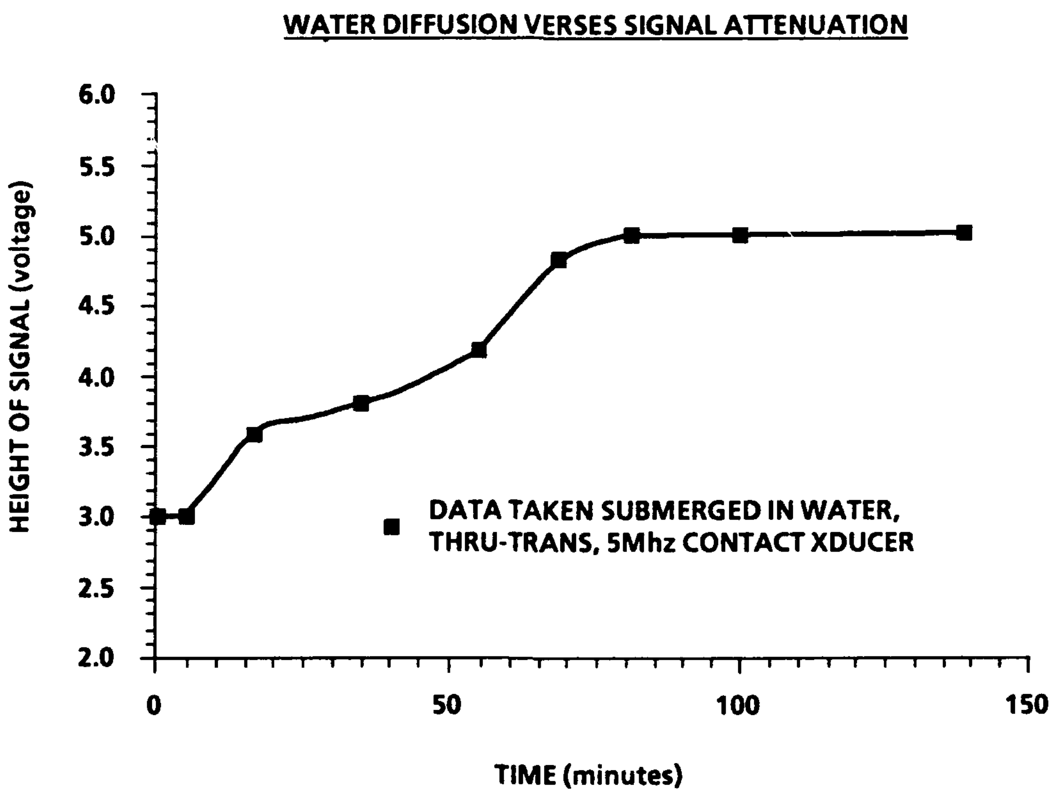

FIGURE A-1. PLOT OF WATER DIFFUSION VERSUS SIGNAL ATTENUATION after 85 min. submerged dB=20 log (V1/V2)=20 log (3.0/5.0)= -4.43 dB

after 35 min. submerged dB=20 log (V1/V2)=20 log (3.0/3.75)= -1.93 dB

From the plot and the data above, the worst case is a change in gain of -4.43 dB after 85 minutes submerged under water. But an ultrasound C-scan takes approximately 35 minutes which has a change in gain of -1.93 dB for this sample. The C-scans of the graphite aluminum composite radiator with the silicone adhesive applied had a change in gain of 6 to 9 dB in the panel after the holes were machined. The change of gain is very high and if attributed to water diffusion only approximately -1.93 dB of the 6 to 9 dB can be accounted for. But, the -1.93 dB of change is without the silicone adhesive leaving a path free for the water to penetrate the composite. Therefore, the 1.93 dB change is highly exaggerated and the 6 to 9 dB change in gain must be due to another phenomenon or a combination of phenomena.

DISTRIBUTION

	Copies
Office of Director of Defense Research and Engineering	
Attn: J. Persh	1
Staff Specialist for Materials and Structures	
Room 3D1089, The Pentagon	
Washington, DC 20301	
Office of Naval Technology	
Attn: W.T. Messick	1
800 N. Quincy Street	
Arlington, VA 22217-5000	
Advanced Submarine Technology Office	
Attn: J. Kelly	1
1515 Wilson Blvd., Rm 705	
Arlington, VA 22209	
Department of the Navy	
Strategic Systems Project Office	
Attn: B.W. Hannah, SP 272	1
Crystal Mall No. 3	
Washington, DC 20362	
Office of Naval Research	
Attn: R. Pohanka, Code 1131	1
Y. Rajapakse, Code 1132SM	1
800 N. Quincy Street	
Arlington, VA 22217-5000	
Commander	
Annapolis Facility	
Naval Surface Warfare Center	
Attn: A.G.S. Morton, Code 2813	1
Annapolis, MD 21402	
Commander	
Naval Air Development Center	
Attn: T.E. Hess, Code 6043	1
G. London, Code 606D	1
I. Shaffer, Code 60C	1
Warminster, PA 18974	
Naval Research Laboratory	
Attn: M.A. Brown, Code 8240	1
W.R. Braun, Code 8221	1
W. Simon, Code 8241	1
4555 Overlook Avenue, S.W.	
Washington, DC 20375	
Commanding Officer	
Naval Underwater Systems Center	
Attn: B. Sandman, Code 3636	1
Newport, RI 02840	
Naval Intelligence Support Center	
Attn: M.E. Andrasco	1
4301 Suitland Road	
Washington, DC 20390	
DPRO, Sunnyvale	
Attn: B. Galligan, SPL 312	1
Lockheed Bldg. 181	
Sunnyvale, CA 94086	
Metal Matrix Composites Information Analysis Center	
Kaman Tempo	
Attn: W. McNamara	2
816 State Street	
P.O. Box 1479	
Santa Barbara, CA 93102-1479	

DISTRIBUTION (Continued)

	Copies
Center for Naval Analyses 4401 Ford Avenue Alexandria, VA 22302-0268	1
Commander Naval Ocean Systems Center Attn: P.D. Burke, Code 9322 San Diego, CA 91252-5000	1
Center for Naval Analyses 4401 Ford Ave. Alexandria, VA 22302-0268	1
Strategic Defense Initiative Organization Attn: M. Obal, SDIO/TNK Washington, DC 20301-7100	1
Defense Advanced Research Projects Agency Attn: B. Wilcox Materials Sciences Division 1400 Wilson Blvd. Arlington, VA 22209	1
Wright Laboratory	
Attn: A. Gunderson, WL/MLLN	1
G. Ormbrek, WL/MLLN	1
S. Schwenker, WL/MLLS	1
D.E. Beeler, WL/MLTN	1
V. Johnson, WL/FIBAA	1
L. Kelly, WL/FIBA	1
D. Roselius, WL/SVS	1
Wright-Patterson AFB, OH 45433	
National Aerospace Plane Office	
Attn: F.D. Boensch, ASD/NAF	1
T.M.F. Ronald, ASD/NAF	1
Wright-Patterson AFB, OH 45433-6503	

	Copies
Library of Congress Attn: Gift & Exchange Division Washington, DC 20540	4
Defense Technical Information Center Cameron Station Alexandria, VA 22314	12
Army Foreign Science and Technology Center Attn: J.G. Crider, FSTC/DRXST-MTI 220 7th Street Charlottesville, VA 22901	1
NASA Headquarters/RTM Attn: S. Venneri 600 Independence Avenue, S.W. Washington, DC 20546	1
NASA/Langley Research Center	
Attn: D. Tenney, Code MS188M	1
S. Tompkins, Code 191	1
Hampton, VA 23665-5225	
NASA/Lewis Research Center Attn: H. Gray, Mail Stop 49-1 21000 Brookpark Road Cleveland, OH 44135	1
NASA/Johnson Space Center Attn: L. Leger, Code ES5 Houston, TX 77058	1
Marshall Space Flight Center Attn: E. Engler, Mail Stop EP13 Huntsville, AL 35812	1

DISTRIBUTION (Continued)

	Copies
Department of the Army	
US Army Materials Technology Laboratory	
Attn: A. Levitt, SLCMT-MCD-E	1
P. Smoot, SLCMT-MCD-E	1
Watertown, MA 02172-0001	
Ballistic Missile Defense Materials Program Office	
US Army Materials Technology Laboratory	
Attn: J. Dignam, Bldg. 131	1
Watertown, MA 02172-0001	
Jet Propulsion Laboratory	
Attn: J. Swann for:	
R. H. Smoak, Mail Stop 67-201	1
4800 Oak Grove Drive	
Pasadena, CA 91103	
Sandia National Laboratories	
Attn: Document Control 8214-1 for:	
B.C. Odegard, Div. 8316	1
Livermore, CA 94550	
Amercom, Inc.	
Attn: W. Bustamente for:	
J. M. Shoemaker	1
8928 Fullbright Avenue	
Chatsworth, CA 91311	
DWA Composite Specialties, Inc.	
Attn: M. Van den Bergh for B. Webb	1
21119 Superior Street	
Chatsworth, CA 91311-4393	

	Copies
The Aerospace Corporation	
Attn: J. G. Gee for	
G. Steckel, MS M2/321	1
H. Katzman, MS M2/242	1
G. Hawkins, MS M2/250	1
W. Kao, MS M2/242	
M. Aswani, MS M4/920	
P.O. Box 92957	
Los Angeles, CA 90009-2957	
Research Opportunities, Inc.	
Attn: Arlene Fillius for W. C. Riley	1
2200 Amapola Court, Suite 101	
Torrance, CA 90501	
Materials Sciences Corporation	
Attn: John Kibler for B. W. Rosen	1
930 Harvest Drive, Suite 300	
Union Meeting Corporate Center	
Blue Bell, PA 19422	
The Charles Stark Draper Laboratory	
Attn: Hope M. Coffman for:	
J. Gubbay, MS37	1
555 Technology Square	
Cambridge, MA 02139	
Fiber Materials, Inc.	
Attn: Ron Marek for:	
R.I. Pepper, Director Research & Development	1
Biddeford Industrial Park	
Biddeford, ME 04005	

DISTRIBUTION (Continued)

	Copies
Advanced Composite Materials Corp.	
Attn: Blake C. Morgan for: P. E. Hood	1
1525 S. Buncombe Road	
Greer, SC 29651-9208	
Fiber Materials, Inc.	
Attn: W. Spalsbury	1
666 North Hague Avenue	
Columbus, OH 43204	
American Cyanamid Company	
Attn: Linda Harbuck for D. A. Foster	1
1937 West Main Street	
P.O. Box 60	
Stamford, CT 06904-0060	
Lockheed R&D Palo Alto Research Laboratory	
Attn: Ralph Lewis for F. W. Crossman D93-10/B204	1
3251 Hanover Street	
Palo Alto, CA 94304	
Lockheed California Company	
Attn: Colleen Woods for:	
D. Chellman, D76-31/B63	1
M. A. Steinberg, D03-10/B61	1
P.O. Box 551	
Burbank, CA 91520	
Boeing Aerospace	
Attn: Corinne Campbell for:	
T.S. Luhman, MS 73-09	1
P. Rimbos, MS 82-97	1
P.O. Box 3999	
Seattle, WA 98124-2499	

	Copies
United Technologies Research Center	
Attn: D. B. Belcher for K. M. Prewo	1
R. W. Reed, MS86	1
411 Silver Lane	
East Hartford, CT 06108	
Lockheed Missiles & Space Company, Inc.	
Attn: J. Wagner for:	
A.A. Woods, D50-43/B590	1
W.W. Sable, D62-17/B104	1
R. Dotson, D62-18/B104	1
J.H. Fyten, D62-92/B564	1
J.T. McGrath, D81-32/B157	1
K. Benner, D59-60/B556	1
B.K. Min, D62-17/B104	1
R.D. Torczyner, D59-60/B556	1
P.O. Box 3504	
Sunnyvale, CA 94088-3504	
GE Astro Space Division	
Attn: C. S. Cipoletta for C. Zweben	1
Bldg. 100, Rm M4018	
P.O. Box 8555	
Philadelphia, PA 19101	
McDonnell Douglas Astronautics Corp.	
Attn: E. Hargrette for: L. Cohen	1
5301 Bolsa Avenue	
Huntington Beach, CA 92647	
Hughes Aircraft Company Space and Communications	
Attn: S. Hison for P. Burns, S64/MS A446	1
Los Angeles, CA 90009	

DISTRIBUTION (Continued)

	Copies
Rockwell International Corporation North American Aircraft Operations Attn: R. Aldrich for B. A. Burroughs 201 North Douglas Street El Segundo, CA 90245	1
Ball Aerospace Systems Division Attn: Peter J. Walker for: D. Lemon H.W. Davis P.O. Box 1062 Boulder, CO 80306	 1 1
Aluminum Company of America Alcoa Laboratories Alcoa Technical Center Attn: J. Sapp for T. B. Gurganus Alcoa Center, PA 15069	1
Amoco Performance Products, Inc. Attn: L. Matthews 375 Northridge Road, Suite 600 Atlanta, GA 30350-3297	1
E.I. DuPont Denemours & Company Central Research & Development Dept. Attn: C. Brown for A.K. Dhingra Room D-6005 Wilmington, DE 19898	1
Ketema Attn: W.E. Davis 3611 South Harbor Blvd., Suite 225 Santa Ana, CA 92704	1
General Dynamics (Convair Aerospace Division) Fort Worth Division Attn: V.G. Harris for A. Chaput, MZ5969 P.O. Box 748 Fort Worth, TX 76101	1
Martin Marietta Orlando Division Attn: R. Mellon for W. Meyerer, MP150 P.O. Box 5837 Sand Lake & Kirkman Roads Orlando, FL 32855	1
The Marquardt Company Attn: L. Lee for M. Katcher P.O. Box 201 Van Nuys, CA 91409	1
Sparta, Inc. Attn: B. Stevens for H. Rediess 23041 de la Carlota, Suite 210 Laguna Hills, CA 92653-1507	1
Sparta, Inc. Attn: L. C. Dunbar 9455 Towne Center Drive San Diego, CA 92121-1964	1
Southern Research Institute Attn: D. Denton for H.S. Starrett P.O. Box 55303 Birmingham, AL 35255	1

DISTRIBUTION (Continued)

	Copies
Textron Specialty Materials Attn: L. Grumer for P.R. Hoffman Two Industrial Avenue Lowell, MA 01851	1
Advanced Materials Laboratory Attn: Tom Altshuler 110 Hillcrest Road Concord, MA 01742	1
COMSAT Corporation Attn: Ron Kessler 22300 Comsat Drive Clarksburg, MD 20871	1

Internal Distribution:

E231	2
E232	3
R30 (C. Mueller)	1
R32 (P. Hesse)	1
R32 (J. Foltz)	10
R32 (A. Bertram)	1
R32 (J. Tydings)	1
R32 (R. Garrett)	1
R32 (J. Clark)	1
R34 (C. Anderson)	1
R34 (J. Liu)	1
R34 (R. Lee)	1
R34 (N. Feldman)	20
R34 (J. Warren)	1
R34 (P. Brown)	1
R34D (C. Blackmon)	1
K205 (W. Messick)	1
K22 (E. Becker)	1
C72W (R. Johnson)	1
E342 (GIDEP)	1

REPORT DOCUMENTATION PAGE	Form Approved OMB No. 0704-0188

1. AGENCY USE ONLY *(Leave blank)*	2. REPORT DATE	3. REPORT TYPE AND DATES COVERED
	December 1991	

4. TITLE AND SUBTITLE
Nondestructive Evaluation of a Graphite Aluminum Composite Space Radiator Panel

5. FUNDING NUMBERS

6. AUTHOR(S)

Neil M. Feldman and John V. Foltz

7. PERFORMING ORGANIZATION NAME(S) AND ADDRESS(ES)
Naval Surface Warfare Center
Dahlgren Division, White Oak Detachment
10901 New Hampshire Ave.
Silver Spring, MD 20903-5000

8. PERFORMING ORGANIZATION REPORT NUMBER
NAVSWC TR 91-492

9. SPONSORING/MONITORING AGENCY NAME(S) AND ADDRESS(ES)

10. SPONSORING/MONITORING AGENCY REPORT NUMBER

11. SUPPLEMENTARY NOTES

12a. DISTRIBUTION/AVAILABILITY STATEMENT

Approved for public release; distribution is unlimited.

12b. DISTRIBUTION CODE

13. ABSTRACT *(Maximum 200 words)*
Graphite aluminum composites which employ graphite fibers for mechanical reinforcement have applications in the aerospace industry. They are particularly attractive for spacecraft thermal management systems due to their ability to efficiently transport heat. The detection and evaluation of damage in structures fabricated from this material is necessary to the efficiency and application of these materials.

This technical report presents research on a graphite fiber reinforced aluminum composite space radiator panel. The panel was evaluated after each of four fabrication stages by four nondestructive techniques: ultrasound, x-ray, dye penetrant, and visual inspection. The results illustrate the importance of nondestructive evaluation (NDE) from the time the composite is fabricated through the time it is implemented into the spacecraft. These NDE technologies will help detect external or internal irregularities (anomalies) at each increment of the fabrication and qualification testing of the composite radiator panel.

14. SUBJECT TERMS

Nondestructive Evaluation
Graphite Aluminum Composite

15. NUMBER OF PAGES
55

16. PRICE CODE

17. SECURITY CLASSIFICATION OF REPORT	18. SECURITY CLASSIFICATION OF THIS PAGE	19. SECURITY CLASSIFICATION OF ABSTRACT	20. LIMITATION OF ABSTRACT
UNCLASSIFIED	UNCLASSIFIED	UNCLASSIFIED	SAR